HYDROMORPHOLOGICAL DYNAMICS OF CANADIAN ARCTIC DELTAS : AN HYDROLOGICAL MODEL OF THE COPPERMINE DELTA.

L. Lafosse[1], J. Stolle[1], S. Coulombe[2], S. Binette[3], N. Canham[1], R. Akana[4], D. Didier[3]

Climate change has transformed coastal and deltaic environments in the Arctic with warmer temperatures, loss of sea ice, higher water levels, and larger storm events. Coastal retreat rates have been measured over 10 m per year in Canadian Arctic severely affecting Indigenous communities. This paper presents one of the first hydrodynamic models of an Arctic delta to better understand the processes specific to the Arctic. The hydrodynamic model has been calibrated and validated with water level and current velocity field measurements in summer 2022. Water levels are well predicted during both calm weather and storm events. A correlation between water level and permafrost erosion at cliff foot is analyzed with a parameter called erosion potential. The erosion potential has been defined as the number of days for which the water level at Graveyard is above the threshold of 0.1 m divided by the total number of days during summer. According to water level measurements from 2021 to 2024, the erosion potential is stochastic across years, with a significant increase in mean water level in 2023, followed by a drop in 2024. Following IPCC projections for sea-level rise, erosion at the foot of Graveyard cliff could occur one out of two days during the summer season in 2050 and every day in 2100. Based on our recent field studies, the aim of this project is to analyze the extent to which hydro-morphodynamic models without considering thermal exchanges can be applied to Arctic coastal engineering. Correctly predicting the impact of climate change in the Arctic will enable better adaptation of local communities in the future.

Keywords: arctic; delta; hydrodynamic modelling; Delft3DFM; erosion

INTRODUCTION

Indigenous communities along Arctic coastlines are becoming increasingly vulnerable to climate change and the impacts of storms (Archer et al. 2017; Ford et al. 2021). Throughout the Arctic, infrastructure, such as houses, schools, roads, airstrips and numerous archaeological sites, have already been eroded/flooded or are under serious threat (Irrgang et al. 2018; Liew et al. 2022). Warmer air, water and permafrost temperatures, higher water levels and waves, increase in precipitation and discharge have altered the hydro-morphological dynamics of Arctic coastlines and deltas (Box et al. 2019). As a result, some permafrost coastal retreat rates have been measured over 10 m per year in Canada (Obu et al. 2016), in Alaska (Jones et al. 2018) and in Russia (Günther et al. 2015). Although mean annual erosion rates were lower, some localized extreme events severely eroded the coastline exceeding 19 m/year in Varandey (Sinitsyn et al. 2019) and 22.3 m/year in the Lena delta in Russia (Fuchs et al. 2020). The majority of permafrost coastlines erosion takes place during the summer months, due to the protection of sea ice during the winter (Chan et al. 2022).

Coastal erosion adaptation projects are beginning to emerge in the Arctic, with hard infrastructure such as dykes, breakwaters and rock revetments, and soft solutions, such as beach nourishment, dune stabilization and infrastructure retreat (Liew et al. 2020). However, the coastal protection measures already in place are described as incomplete and short-term (Smith and Sattineni 2016), sometimes forcing communities to relocate (Albert et al. 2017). Both local communities and scientists agree on the need for protection and adaptation projects (Magnan et al. 2022). However, a lack of knowledge about the processes causing erosion of permafrost coastlines has limited the effectiveness of traditional engineering protection methods. With a better understanding of these hydro-morphological dynamics and the impact of climate change, new hard and soft methods could be developed and discussed with local communities in the Arctic.

387 Arctic deltas have been inventoried and classified according to their hydrodynamic forcing: river, tidal or wave dominated, as for deltas in temperate environment. Nevertheless, Arctic delta morphodynamics can vary widely due to differences in ice cover and sediment fluxes related to the presence of permafrost (Overeem et al. 2022). However, few studies, combine delta dynamics with processes specific to permafrost dynamics, and this is hindered by a lack of field data and hydro-morphological models suited to the region (Frederick et al. 2016). Some are using hydro-morphodynamic models based on physical equations (Bull et al. 2020) but with a low spatial resolution of 100 m for the hydrodynamic part around the coast. Other studies modelled the hydrodynamics with a reduce complexity approach (Chan et al. 2022) without considering oceanographic processes such as tides and waves. However, water level variability in an estuary depends on several processes with constructive or destructive interactions with each other: mean sea level, tides, atmospheric surge, river discharge, waves and wave set up (Krien et al. 2017; Pertiwi et al. 2021). Tide-surge interactions, also called still water

[1] Centre Eau Terre Environnement, INRS, Québec, Québec, Canada
[2] Polar Knowledge Canada, Cambridge Bay, Nunavut, Canada
[3] Département de biologie, chimie et géographie, UQAR, Rimouski, Québec, Canada
[4] Hamlet of Kugluktuk, Kugluktuk, Nunavut, Canada

level, are defined as the interactions between mean sea level, tides and wind-driver surge (Idier et al. 2019). Wind-driver storm surge cannot be neglected in shallow water areas and could lead to extreme water levels causing flood hazards in deltas (Eilander et al. 2020). Tide-surge interactions could increase extreme water level up to 1 m (Krien et al. 2017) whereas the addition of waves can also contribute to flood hazards but have less effect on extreme water level (Idier et al. 2019). Furthermore, the projected flood hazards due to extreme water levels need to consider the sea level rise, up to 1.01 m in 2100 with the extreme scenario according to the IPCC 6th Assessment Report (Fox-Kemper et al. 2021; Garner et al. 2021). Current numerical models are unable to assess the processes behind the erosion of permafrost shoreline due to storm impacts in an Arctic delta and predict the hydro-morphological dynamic depending on climate change scenarios.

AIM AND APPROACH

The long-term objective of this project is to provide a basis for improving numerical models of Arctic deltas on a local scale of a few dozen kilometers. To address the concerns of the community of Kugluktuk about morphodynamic changes in the Coppermine delta in Nunavut (Canada), this study aims to:

1. Calibrate a hydrodynamic model of the Coppermine Delta in Canadian Arctic;
2. Validate the hydrodynamic event with a storm event;
3. Analyze the impact of sea level change on erosion risk.

This study takes into account the river and ocean hydrodynamics with water level and current velocity measurements from field surveys from summer 2021 to 2024. Local anthropogenic impacts are considered insignificant compared to other environmental changes in the Arctic, nor biological processes. The presence of ice (break-up, plug, floating ice), which is absent in summer in the Coppermine Delta, is not considered in the model. Heat transfer, although assumed to be relevant to understanding the dynamics of an Arctic delta, is not included at this stage of the project. Thus, this study will provide a basis for modelling morphological dynamics and sediment transport in the delta, and for assessing the impact of thermal processes on morphological changes.

STUDY AREA

The Hamlet of Kugluktuk (ᖁᔭᓐᓄᖅ, meaning "Place of moving water") is located on the north coast of mainland Canada in the Kitikmeot administrative region of Nunavut (latitude: 67° 49′N and longitude: 115° 07′W) (Wilson et al. 2021). At the mouth of the Coppermine River and Coronation Gulf, the community of 1382 inhabitants (from the 2021 census) is on the western edge of the Coppermine delta. The highest point is 170 m above sea level, at the top of a rocky hill (Smith 2014). By 2100, isostatic uplift would be around 23 cm higher, and relative sea level rise is expected to be between -20 and +65 cm depending on climate change scenarios (James et al., 2011). In 2007 and 2009, community surveys highlighted vulnerability to weather changes (ice, precipitation, wind, temperature) and to infrastructure degradation due to permafrost freezing/thawing cycle (Prno et al. 2011; Smith 2014). A climate change adaptation plan was drawn up with the community (Johnson and Arnold 2010). Nevertheless, some critical infrastructure such as the port, shown on Smith's (2014) map, are no longer accessible and fishing cabins along the shoreline have been damaged. Due to the decline in water depth making navigation and fish migration difficult in the delta and an increase in shoreline erosion, priority areas for protection and restoration were identified in February 2019 by the Hamlet Council and members of the Hunters and Trappers Organization (Wilson et al. 2021). Coastal erosion is particularly threatening the traditional cemetery located on one of the deltaic islands (Fig. 1). The community's concern about the possible destruction of part of the cemetery is reinforced by the retreat of the coastline visible in aerial photographs and satellite images since 1952 (Binette et al. 2024). Up to now, at least one grave has already fallen into the water. The foot of the cemetery is well protected from offshore waves due to the delta morphology corresponding to a low energy environment with a maximum significative wave height of 0.2 m (Binette et al. 2024).

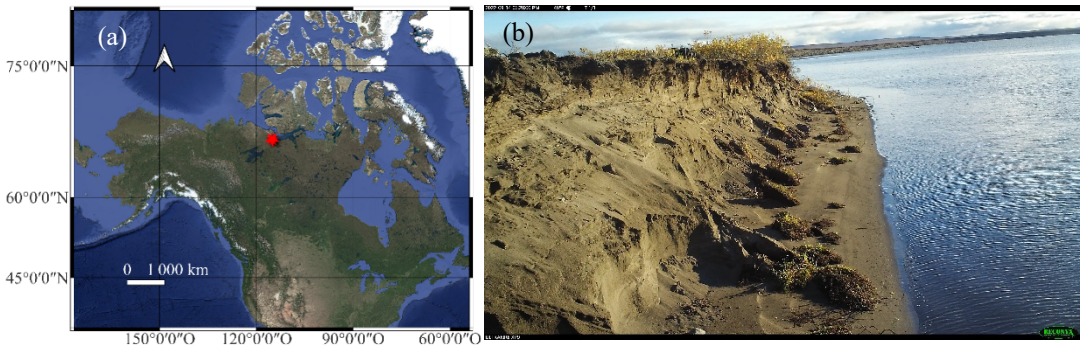

Figure 1. Location of the Coppermine delta in the Canadian Arctic (a) and main region of interest, the Graveyard Island where the traditional cemetery is on the top of cliff (b).

METHODOLOGY

Field measurements

Community-based field surveys were carried out during the summer months from 2021 to 2024 from July to October in the Coppermine Delta. Pressure sensors (RBR Virtuoso, recording total pressure continuously at 4 Hz) and ADCPs were used for the model calibration and validation in 2022 (Table 1). Water levels are determined considering hourly atmospheric pressure from the weather station at Kugluktuk airport. Water in the delta was always considered fresh due to the low salinity < 0.1 ppt measured with an RBR CTD sensor in summer 2021. Current velocity was measured from two types of ADCP sensors: ADCP Nortek Eco Current Profiler (called ADCP ECO) and ADCP Nortek Signature 1000. For both ADCPs, the current velocity was automatically processed by Nortek software and was averaged in the water column every 20 min and converted in ENU coordinates. In the river, the daily discharge was calculated from the current velocity daily averaged at River upstream multiplied by the estimated cross-sectional area of 634 m². The cross-sectional area corresponds to an approximation of the surface between bed level determined from the bathymetric map and the water level considered constant at z = 0 m. The location of each sensor and the bathymetric measurements were determined in NAD83 UTM zone 11N (EPSG: 2955) with the CGVD2013 datum.

Table 1. Hydrodynamic sensors characteristics.

Instruments	Location	Sampling rate [Hz]	Deployment [mm/dd/yyyy]	Recovery [mm/dd/yyyy]
RBR Virtuoso D	Graveyard	4	07/08/2022	10/06/2022
Nortek ADCP Signature1000	Graveyard	2	07/06/2022	07/15/2022
Nortek ADCP Eco Current Profiler	River upstream	0.008	07/06/2022	07/15/2022
Nortek ADCP Eco Current Profiler	River upstream	0.003	07/17/2022	10/05/2022

A bathymetric survey campaign was conducted in July 2022 with a single beam eco-sounder (HydroBall® buoy) that can measure to a minimum water depth of 0.1 m. The data collected was validated by the Canadian Hydrographic Service (CHS) quality analysis procedure (Anon. 2020) with 771 intersections and a vertical error of less than 0.4 m for 98.8 % of the measurements. The bathymetric map used in the model was constructed by combining field measurements; a satellite derived bathymetric map produced by two Sentinel-2 images (10 m spatial resolution) in 2022 (2022-08-01 and 2022-08-06) including tidal correction produced by the ARCTUS AI-assisted empirical model; and open access data: ArcticDEM (https://fridge.pgc.umn.edu/) (2 m spatial resolution) and Canadian Hydrographic Service Non-Navigationnal NONNA (https://data.chs-shc.ca/dashboard/map) (10 m spatial resolution). Due to a lack of data in the North-East region, new offshore points of 50 m depth were created. Interpolation method k-nearest neighbours regressor depending on 3 neighbors and considering a uniform weight between each neighbor was applied by splitting the map into 5 areas and then over the whole map. The bathymetric map was interpolated on the model's mesh with a triangular interpolation and was compared with 2023 RTK GPS field measurements. A relatively low correlation is shown with a R^2 equal to 0.38, a RMSE of 0.41 m and a bias of 0.3 m. Considering the bathymetric map with a 10 m spatial resolution and many sand bars at this depth, the bathymetric map interpolated on the mesh of the model is considered acceptable (Fig. 2).

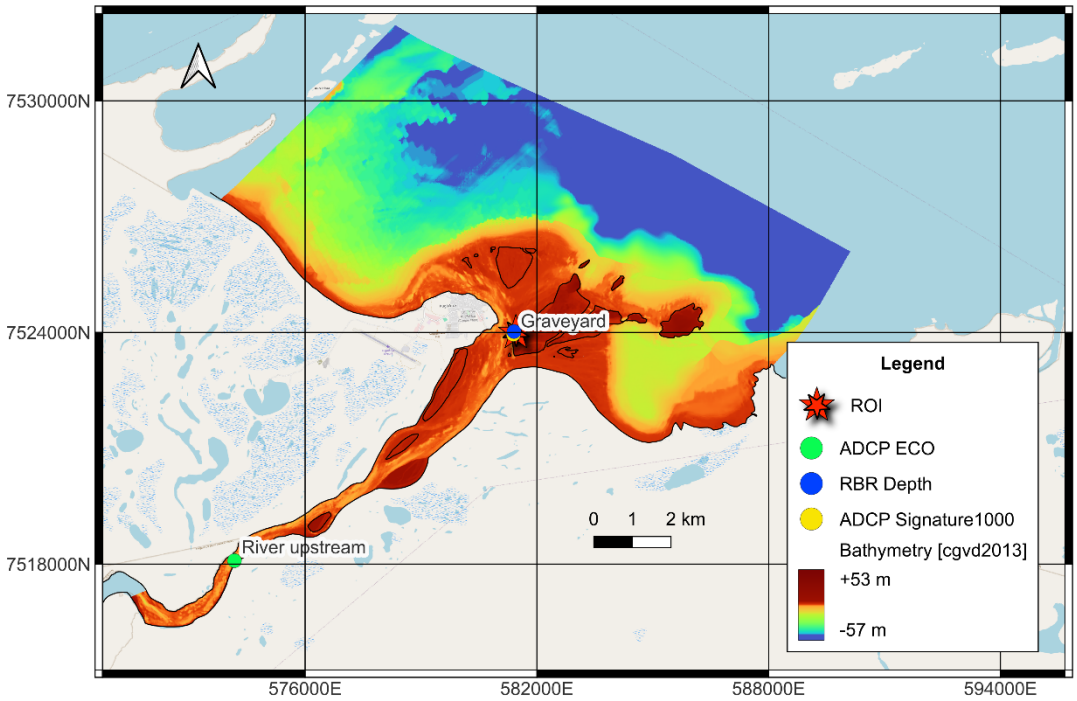

Figure 2. Bathymetric map of the Coppermine delta including the ADCP sensors and a pressure sensor (RBR) at River upstream and along Graveyard Island.

Model set up

The hydro-morphological model was implemented using Delft3D FM software (https://oss.deltares.nl/web/delft3d), widely used tool for simulating deltaic evolution in temperate environments (Edmonds et al. 2021). The Delft3D FM software module D-FLOW was used, which simulates multi-dimensional hydrodynamic circulation and transport dynamics including sediments transport. In this model, we focus on the hydrodynamics of the delta in 2D, with particular emphasis on the region of interest Graveyard. The model solves the 2D shallow-water equations derived from the Navier-Stokes equations for an incompressible fluid in the horizontal plane The averaged depth assumption could be applied due to the shallow bathymetry and the limited stratification based on salinity measurements from 2021. Delft3D has been widely used to model delta dynamics, and the 2D model can provide accurate results while reducing computing power and time (Tejedor et al. 2016; Braat et al. 2017; Lenstra et al. 2019). We assume anisotropic turbulent viscosity and hydrostatic pressure. The effect of the Coriolis force was neglected. Wave and wind processes were considered negligible for the following hydrodynamic model.

In Cartesian coordinates, seven different triangular flexible mesh were tested around same spatial resolution of 440 m offshore and 27 m in the river with different resolution closed to Graveyard. To ensure the model's stability, all the grids were orthogonalized (<= 0.001) and smoothed. The boundary conditions were defined hourly as the discharge in the river upstream and the water level offshore. All the model parameters were described in Table 2 and the other parameters were set as default. All the simulations were run in parallel with six partitions. The model results were independent from the initial water level. A robust sensitivity analysis was carried out to identify the best-performing mesh spatial resolution. Then, sensitivity analysis of the viscosity, diffusivity and Manning's coefficients were conducted for the model's calibration from 07/09/2022 to 07/12/2022 which allows the simulation of several tidal cycles. The best suitable parameters have been selected and validated from 07/14/2022 to 07/17/2022 during a storm event including one of the highest water levels measured at Graveyard in summer 2022.

Table 2. Model parameters in D-Flow FM module

Parameters	units	Selected
Mesh spatial resolution (at Graveyard)	m	2-18
Horizontal eddy viscosity	m^2/s	0.01-10
Horizontal eddy diffusivity	m^2/s	0.1-10
Manning friction coefficient	$s/m^{1/3}$	0.015-0.035
Salinity	ppt	0
Water temperature	°C	18
Uniform bed level (if no data)	m	-1.5
CFL	-	0.7
Maximum time step	s	30

Model parameters were evaluated on the Root Mean Square Error (RMSE), the correlation coefficient R^2, the coefficient of determination r and the bias according to:

1. Water level, with the most accurate possible predictions at Graveyard in 2022. Current velocities at Graveyard were close to 0 m/s and it is assumed that water level variation mainly controls erosion at the foot of Graveyard.
2. Current velocities towards East and North, with the most accurate predictions possible at River upstream in 2022. Current velocities in River upstream are essential for sediment transport, which will be studied later.

Erosion potential

Storms events were analyzed at Graveyard Island from the 8th of July to the 29th of September from 2022 to 2024 with the Peaks-Over-Threshold (POT) method (Bocharov 2023) applied on water level field measurements. Extreme values were selected above a threshold of 0.1 m. This threshold was determined according to the water level during events generating erosion visible at the Graveyard bluff foot. Erosion events were analyzed from time-lapse cameras in the report from Binette et al. (2024). A minimum time between two events of 24 h is considered to ensure event independence (Kim et al. 2021). The erosion potential was calculated as the number of days for which the water level is above the threshold of 0.1 m divided by the total number of days from the 9th of July to the 29th of September for each year. This method has been used by Anderson et al. (2021), who calculated the number of days per year that water level exceeded a threshold to study the overtopping prediction of a berm.

The most recent regional projections of sea-level change were provided by the IPPC sixth Assessment Report (AR6) (Fox-Kemper et al. 2021; Garner et al. 2021) available on the NASA sea-level projection tool (https://sealevel.nasa.gov/ipcc-ar6-sea-level-projection-tool). The water level change was relative to the water level between 1995 and 2014 and depend on the region, in our case latitude 68° N and longitude -114° E. Three scenarios were selected SSP2-4.5, SSP3-7.0 and the highest water level scenario SSP5-8.5 from 2020 to 2100 with a medium confidence interval (Fig. 3). To analyze erosion potential due to project sea level rise, a bias was added on the total water level measured during summer 2022 at the offshore boundary depending on IPCC scenarios. The addition of a sea level bias on water level is similar to the projection of annual high tides depending on IPCC scenarios by Idier et al. (2019).

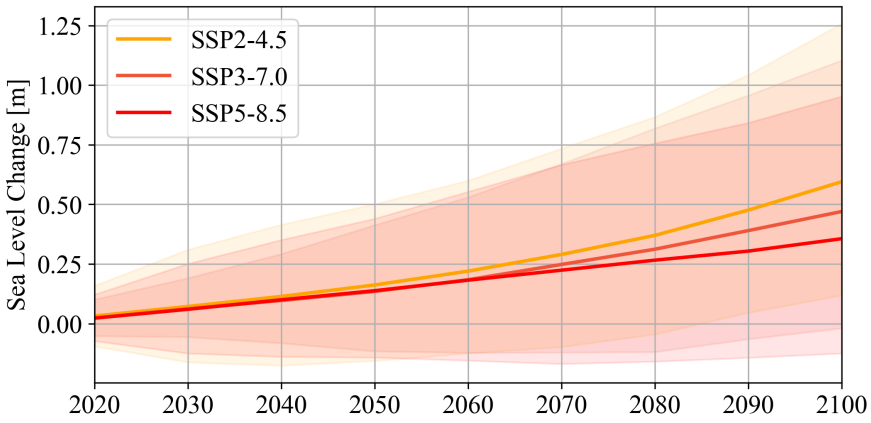

Figure 3. Median sea-level change projections [m] near the Coppermine Delta (lat : 68°, lon:-114°) from 2020 to 2100 according to IPPC AR6 for 3 scenarios : SSP2-4.5, SSP3-7.0, SSP5-8.5. Shaded areas correspond to the 5th–95th percentile ranges for each scenario.

RESULTS

Model Calibration

Among the seven triangular flexible mesh grids tested, statistical analyses of three grids are presented from the coarsest to the finest spatial resolution (Table 3). The characteristic length (L_c) of a cell is considered as the average length of a triangle. The characteristic length at River upstream was equal to 27 m for each grid. Mesh spatial resolution varied especially at Graveyard location with a characteristic length between 3.7 m to 30 m.

Table 3. Characteristics of 3 triangular flexible mesh grids including for each grid the minimum characteristic length ($L_{c,\ min}$), the maximum characteristic length ($L_{c,\ max}$), the characteristic length at Graveyard ($L_{c,\ graveyard}$) and the number of elements.

Grids	$L_{c,\ min}$	$L_{c,\ max}$	$L_{c,\ graveyard}$	Number of elements
Grid 1	17.5	464	30	140 682
Grid 2	3.1	447	7.5	460 070
Grid 3	2.1	447	3.7	556 180

The statistical analysis (Fig. 4) confirmed all the grids correctly predict water level, with an average R^2 greater than 0.8 at Graveyard and River upstream. The grid chosen for the further analysis was grid 2, with a better correlation for current velocities at River upstream. However, all the grids have shown a poorer correlation for current velocity at Graveyard. With the Grid 2, the current velocity at Graveyard had a correlation coefficient about 0.56 towards East and 0.31 towards North.

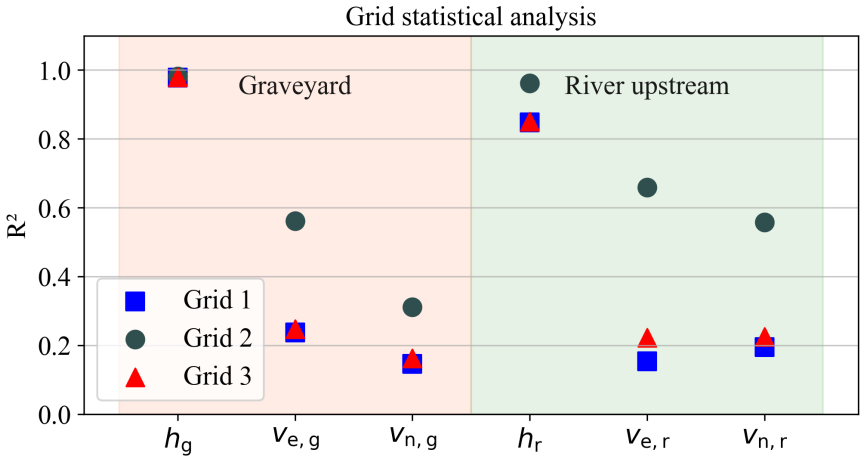

Figure 4. Grid statistical analysis with the correlation coefficient R^2 at Graveyard and River upstream depending on water level (h_g and h_r respectively), velocity towards East ($v_{e,g}$ and $v_{e,r}$) and velocity towards North ($v_{n,g}$ and $v_{n,r}$).

Several model parameters were tested and the parameters with the best predictions for water level and current velocity were selected depending on RMSE and R^2 analysis (Table 4). The other model parameters were left at their default values.

Table 4. Model parameters tested and selected in D-Flow FM module

Parameters	unit	Default	Tested	Selected
Horizontal eddy viscosity	m^2/s	0.1	0.01 ; 0.1 ; 1 ; 5 ; 7 ; 10	0.1
Horizontal eddy diffusivity	m^2/s	0.1	0.1 ; 1 ; 5 ; 10	0.1
Manning friction coefficient	$s/m^{1/3}$	0.023	0.015 ; 0.017 ; 0.2 ; 0.023 ; 0.026 ; 0.028 ; 0.035 ; variable [0.015-0.035]	0.015

Horizontal eddy diffusivity and viscosity calibration had no significant improvement in prediction; thus, the default values have been chosen. The impact of Manning coefficient on current velocity at Graveyard and River upstream is presented on Fig. 5. For constant Manning's coefficients, the simulation with R^2 closest as possible to 1 is better with 0.015 $s/m^{1/3}$ for current velocity at River upstream and, in

contrast, the largest Manning coefficient of 0.035 provides a better prediction at Graveyard. The result of a variable Manning coefficient equal to 0.015 s/m$^{1/3}$ at River upstream and 0.035 s/m$^{1/3}$ at Graveyard and offshore improve slightly the general prediction but the current velocity at River upstream is less well predicted than the results with the one constant of 0.015 s/m$^{1/3}$. Considering the current velocity at River upstream, the subsequent analysis will use a Manning coefficient constant equal to 0.015 s/m$^{1/3}$ (Table 5).

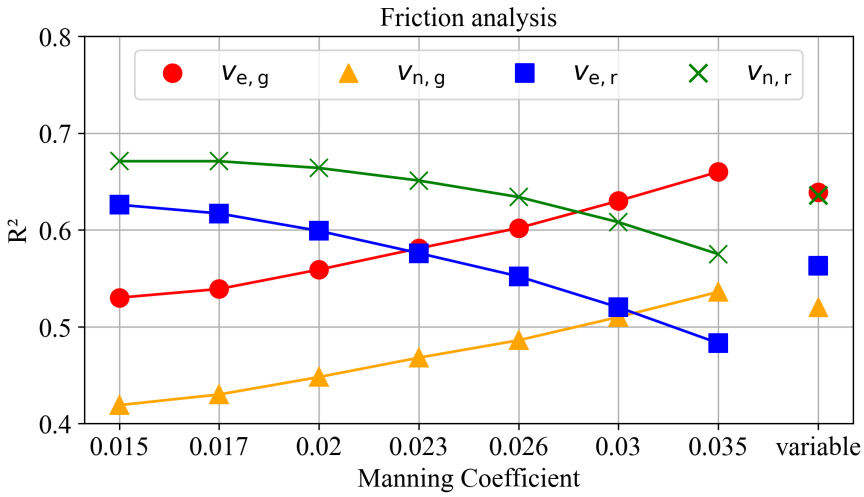

Figure 5. Correlation coefficient R² compared with manning coefficient for the velocity towards East and North at Graveyard and River upstream. The statistics are calculated for a 3-day simulation period from 07/09/2022 to 07/12/2022 during a period considered without storm event.

Model Validation

The analysis for the calibration period from 07/09/2022 to 07/12/2022 and during a storm event for the validation period from 07/14/2022 to 07/17/2022 are presented in the Table 5. The time series of model prediction avec field measurements for water level and current velocity towards East and North at Graveyard and at River upstream are shown for the validation period on the Fig. 6.

Table 5. Statistical analysis with the selected parameters depending on water level at Graveyard (h_g) and velocity towards East ($v_{e,r}$) and velocity towards North ($v_{n,r}$) at River upstream for a 3-day calibration period and for the validation the first 3-day storm event in July 2022.

Statistics	Calibration			Validation		
	h_g	$v_{e,r}$	$v_{n,r}$	h_g	$v_{e,r}$	$v_{n,r}$
RMSE	0.01	0.02	0.04	0.02	0.03	0.03
R^2	0.98	0.63	0.67	0.99	0.51	0.45
r	0.99	0.80	0.82	0.99	0.71	0.67
bias	0.002	-0.006	0.037	0.000	-0.028	0.011

The water level at Graveyard is well predicted for the model calibration and the validation. During the storm event of the validation period, the model is able to predict the water level rise as measured in the field at Graveyard and at River upstream. The current velocity predictions are considered acceptable at River upstream, therefore the fluctuation during the storm is not predicted and the velocity towards North are overestimated by the model especially during the calibration period. The current velocity towards North and East at Graveyard are variable in the field measurements and closed to 0 m/s. However, the model cannot predict the current velocity, especially towards East for which the prediction and the measurements are in the opposite direction.

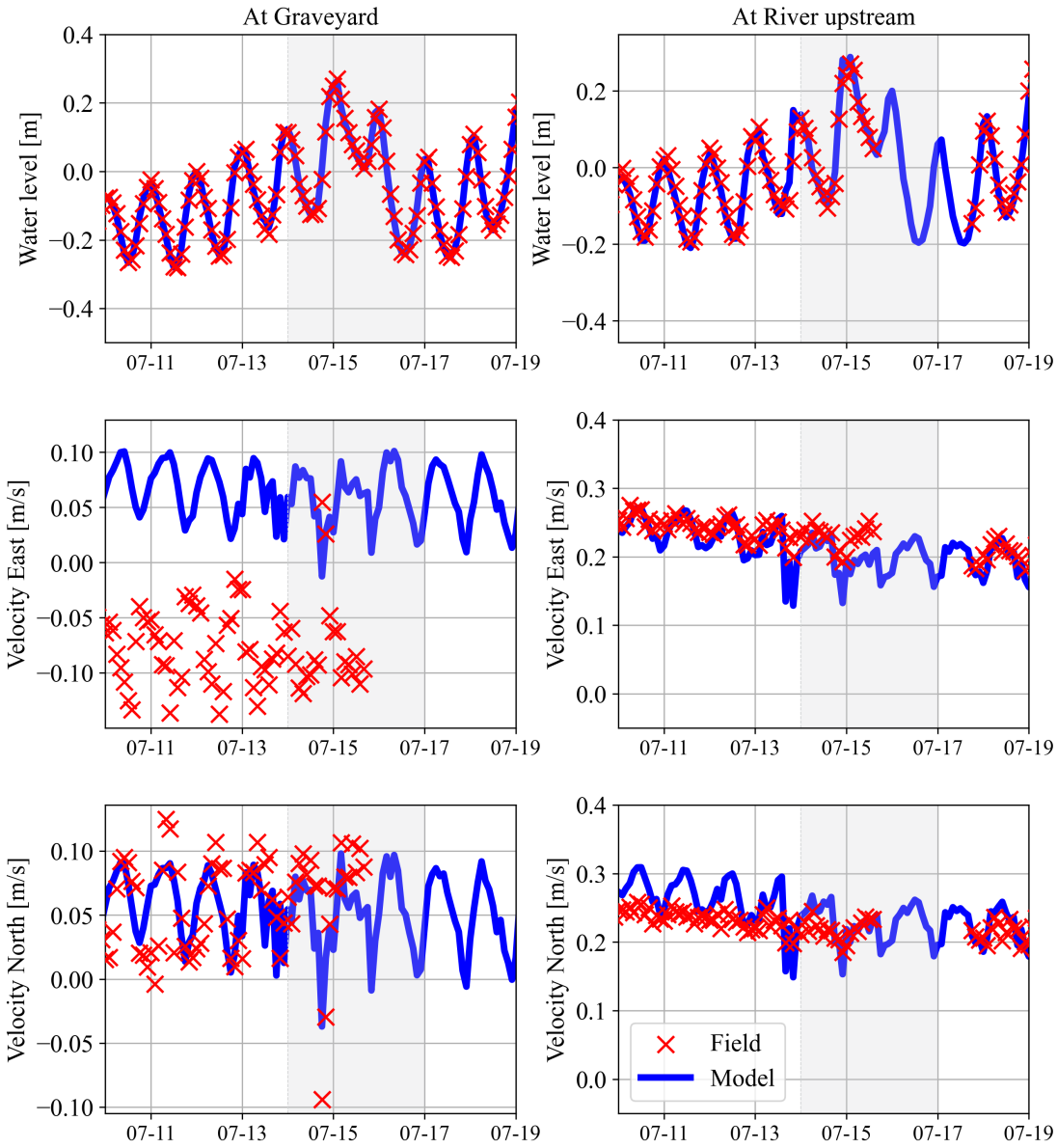

Figure 6. Time series of the water level, velocity towards East and North at Graveyard (left panels) and at River upstream (right panels) with the field measurements in red cross and the model prediction in blue line during a storm event for the validation period from 07/14/2022 to 07/17/2022 (in light gray). Except for the water level measurements at Graveyard, no sensor was deployed between 07/16/2022 and 07/18/2022.

Erosion Potential

From water level measurements at Graveyard, 6 storm events causing potential erosion have been identified, corresponding to 20 days with a maximum water level higher than 0.1 m from 07/09/2022 to 09/29/2022 (Fig. 7). For the same period, the model estimates 19 days, one day inferior to the field measurements which proves the good model estimation of water level.

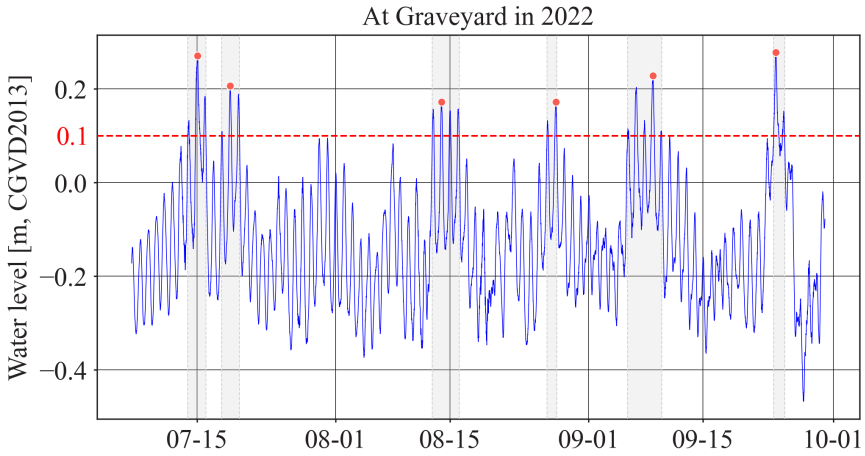

Figure 7. Water level at Graveyard during summer 2022 field measurements with the threshold of 0.1 m in red dash line, the peak extreme values in red dots and the grey shaded areas for each event.

The erosion potential (Fig. 8) at Graveyard increases significantly when the water level rises. An average 0.1 m rise in water level means that one out of two days the foot of the cliff is eroded during the summer period. In 2022, the model prediction as well as the field measurements show an erosion potential of 0.23. The erosion potential is not linear across years, with a significant increase in mean water level seen in 2023, followed by a drop in 2024. In summer 2023, the field measurements show an average water level increase of 0.08 m compared to the summer 2022. 15 storm events for a total of 31 days above the threshold have been recorded during the summer 2023 field campaign, equal to a probability of 0.38. However, the scenario SSP2-4.5 predicts an average rise of water level in 2023 about 0.004 m compared to 2022 corresponding to a probability of 0.23, same than in 2022. In summer 2024, the average water level in the field drops of 0.03 m compared to 2022. 7 storm events have been identified with 7 days out of 83 days above the threshold.

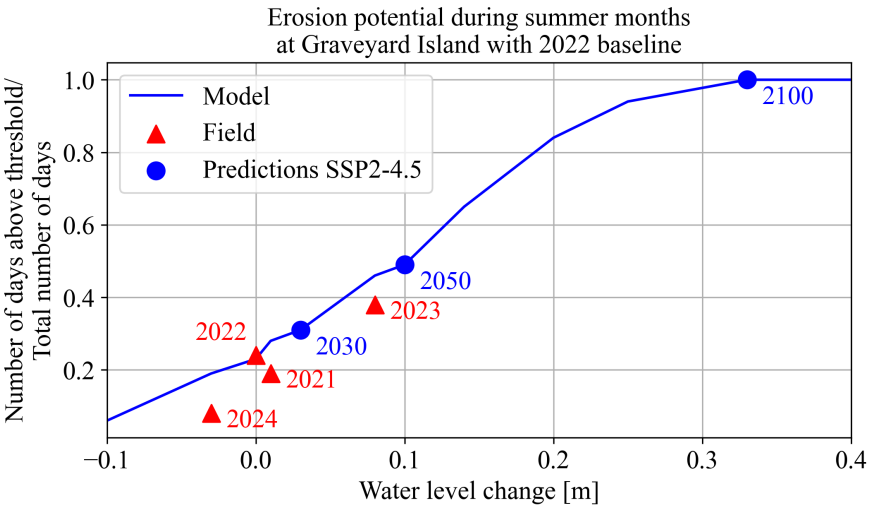

Figure 8. Erosion potential at Graveyard Island depending on water level change [m] (blue line) as a bias added on the water level field measurements from 07/09/2022 to 09/29/2022. The erosion potential is calculated as the number of days for which the water level is above the threshold of 0.1 m divided by the total number of days. The erosion potential is predicted in 2030, 2050 and 2100 for the scenario SSP2-4.5 (blue dot) and calculated from field measurements during summer months from 2021 to 2024 (red triangles).

The IPCC projections of sea level rise expect an average median increase of 0.1 m in 2050 with the scenario SSP2-4.5 corresponding to an erosion potential of 0.5, meaning erosion at the foot of the cliff

could occur one out of two days during the summer season. In 2100, erosion could occur every day during the summer season if this cliff foot elevation is maintained.

DISCUSSION

The current velocity is relatively well predicted by the model in the correct amplitude range, but its direction was not following the ebb and flood tidal variation unlike the field measurements. In a micro-tidal estuary, the location of current velocity sensor could have an impact on the analysis of model performance (Khanarmuei et al. 2020), as well as the bathymetric map accuracy (Ye et al. 2018). The lower bathymetry precision in some part of the delta could be one of the reasons why the grid giving the best predictions of water level and current velocity is not the grid with the finest spatial resolution. Nevertheless, this model predicts well water levels during both calm weather and storm events, as has also been demonstrated with larger tidal amplitude in embayments on Prince Edward Island (Manson et al. 2015).

The water level seems to be the most relevant hydrodynamic parameter to induce erosion, especially when water level rises. With sea level rise projections, the frequency of extreme events could increase more rapidly considering the interactions between tides, storm surge, wave setup and sea level rise (Idier et al. 2019). Like in the Coppermine delta, unprecedented summer storms are recorded in the Arctic with significant increase in water level (Yamagami et al. 2017), accentuating the risk of erosion and delta flooding in the Arctic deltas (Forbes et al. 2022). In the Mackenzie delta, a storm in July 2016 has led to a local increase in water level of 1 m (Scharffenberg et al. 2019). Nevertheless for long-term predictions, the isostatic adjustment has not been considered in the erosion potential predictions but in 2100, the median relative sea level should decrease up to 0 m in the Coppermine delta for SSP5-8.5 based on the AR5 IPCC report, which is the most detailed study of the Canadian Arctic (James et al. 2021). The impact of high temperature, as measured in the Coppermine delta in 2022 (Binette et al. 2024), could also have a significant impact on permafrost erosion, and so have influenced on morphological change, sediment transport and hydrodynamics in the delta.

CONCLUSION

The hydrodynamic model of the Coppermine Delta has been calibrated and validated with water level and current velocity field measurements in summer 2022. Water levels are well predicted during both calm weather and storm events ($R^2 > 0.98$). The erosion potential has been defined as the number of days for which the water level at Graveyard is above the threshold of 0.1 m divided by the total number of days from the 9th of July to the 29th of September for each year. According to water level measurements from 2021 to 2024, the erosion potential is a stochastic process, with a significant increase in mean water level in 2023, followed by a drop in 2024. Following IPCC projections for sea-level rise, erosion at the foot of Graveyard cliff could occur one out of two days during the summer season in 2050 and every day in 2100. The coastal protection projects of the last 20 years in the Arctic have, at best, been based on hydro-morphodynamic models without considering thermal exchanges. Based on our recent field studies, we are currently analyzing the extent to which these models can be applied to Arctic coastal engineering. Correctly predicting the impact of climate change in the Arctic will enable better adaptation of local communities in the future.

REFERENCES

Albert, S., Bronen, R., Tooler, N., Leon, J., Yee, D., Ash, J., Boseto, D. and Grinham, A., 2017. Heading for the hills: climate-driven community relocations in the Solomon Islands and Alaska provide insight for a 1.5 °C future. *Regional Environmental Change*, 18 (8), 2261–2272.

Anderson, D. L., Ruggiero, P., Mendez, F. J., Barnard, P. L., Erikson, L. H., O'Neill, A. C., Merrifield, M., Rueda, A., Cagigal, L. and Marra, J., 2021. Projecting Climate Dependent Coastal Flood Risk With a Hybrid Statistical Dynamical Model. *Earth's Future*, 9 (12).

Anon., 2020. *General documentation for planning, acquisition and processing of HydroBall ® data User Guide* [online]. Available from: http://www.m2ocean.com/.

Archer, L., Ford, J. D., Pearce, T., Kowal, S., Gough, W. A. and Allurut, M., 2017. Longitudinal assessment of climate vulnerability: a case study from the Canadian Arctic. *Sustainability Science*, 12 (1), 15–29.

Binette, S., Didier, D., Coulombe, S., Akana, R., Jourdain-Bonneau, C., Zouaghi, F., Boisson, A., Lafosse, L. and Stolle, J., 2024. *Coastal Erosion and Shoreline Evolution Analysis in Kugluktuk, Nunavut*.

Bocharov, G., 2023. pyextremes (Version 2.3.3). [online]. Available from: https://github.com/georgebv/pyextremes [Accessed 6 Nov 2024].

Box, J. E., Colgan, W. T., Christensen, T. R., Schmidt, N. M., Lund, M., Parmentier, F. J. W., Brown, R., Bhatt, U. S., Euskirchen, E. S., Romanovsky, V. E., Walsh, J. E., Overland, J. E., Wang, M., Corell, R. W., Meier, W. N., Wouters, B., Mernild, S., Mård, J., Pawlak, J. and Olsen, M. S., 2019. Key indicators of Arctic climate change: 1971-2017. *Environmental Research Letters*, 14 (4).

Braat, L., Van Kessel, T., Leuven, J. R. F. W. and Kleinhans, M. G., 2017. Effects of mud supply on large-scale estuary morphology and development over centuries to millennia. *Earth Surface Dynamics*, 5 (4), 617–652.

Bull, D. L., Bristol, E. M., E.Brown, R.C.Choens, C.T.Connolly, C.Flanary, Frederick, J. M., Jones, B. M., C.A.Jones, M.WardJones, McClelland, J. W., A.Mota and I.Tezaur, 2020. *Arctic Coastal Erosion : Modeling and Experimentation*. Sandia Report.

Chan, N. H., Langer, M., Juhls, B. and ..., 2022. Arctic Delta Reduced Complexity Model and its Reproduction of Key Geomorphological Structures. *Earth Surface …* [online], (June), 1–31. Available from: https://esurf.copernicus.org/preprints/esurf-2022-25/%0Ahttps://esurf.copernicus.org/preprints/esurf-2022-25/esurf-2022-25.pdf.

Edmonds, D. A., Chadwick, A. J., Lamb, M. P., Lorenzo-Trueba, J., Murray, A. B., Nardin, W., Salter, G. and Shaw, J. B., 2021. *Morphodynamic Modeling of River-Dominated Deltas: A Review and Future Perspectives*. Reference Module in Earth Systems and Environmental Sciences.

Eilander, D., Couasnon, A., Ikeuchi, H., Muis, S., Yamazaki, D., Winsemius, H. C. and Ward, P. J., 2020. The effect of surge on riverine flood hazard and impact in deltas globally. *Environmental Research Letters*, 15 (10).

Forbes, D. L., Craymer, M. R., James, T. S. and Whalen, D., 2022. Subsidence drives habitat loss in a large permafrost delta, Mackenzie River outlet to the Beaufort Sea, western Arctic Canada. *Canadian Journal of Earth Sciences*, 59 (11), 914–934.

Ford, J. D., Pearce, T., Canosa, I. V. and Harper, S., 2021. The rapidly changing Arctic and its societal implications. *Wiley Interdisciplinary Reviews: Climate Change*, 12 (6), 1–27.

Fox-Kemper, B., Hewitt, H. T., Xiao, C. and Aðalgeirsdóttir, G., 2021. *Ocean, Cryosphere and Sea Level Change. In: Climate Change 2021: The Physical Science Basis. Contribution of Working Group I to the Sixth Assessment Report of the Intergovernmental Panel on Climate Change*.

Frederick, J. M., Thomas, M. A., Bull, D. L., Jones, C. A. and Roberts, J. D., 2016. *The Arctic Coastal Erosion Problem*. Sandia Report.

Fuchs, M., Nitze, I., Strauss, J., Günther, F., Wetterich, S., Kizyakov, A., Fritz, M., Opel, T., Grigoriev, M. N., Maksimov, G. T. and Grosse, G., 2020. Rapid Fluvio-Thermal Erosion of a Yedoma Permafrost Cliff in the Lena River Delta. *Frontiers in Earth Science*, 8 (August).

Garner, G. G., Kopp, R. E., Hermans, T., Slangen, A. B. A., Koubbe, G. and Turilli, M., 2021. *Framework for Assessing Changes To Sea-level (FACTS). Geoscientific Model Development.*

Günther, F., Overduin, P. P., Yakshina, I. A., Opel, T., Baranskaya, A. V. and Grigoriev, M. N., 2015. Observing Muostakh disappear: Permafrost thaw subsidence and erosion of a ground-ice-rich Island in response to arctic summer warming and sea ice reduction. *Cryosphere*, 9 (1), 151–178.

Idier, D., Bertin, X., Thompson, P. and Pickering, M. D., 2019. Interactions Between Mean Sea Level, Tide, Surge, Waves and Flooding: Mechanisms and Contributions to Sea Level Variations at the Coast. *Surveys in Geophysics*.

Irrgang, A. M., Lantuit, H., Gordon, R. R., Piskor, A. and Manson, G. K., 2018. Impacts of past and future coastal changes on the yukon coast — threats for cultural sites, infrastructure, and travel routes. *Arctic Science*, 5 (2), 107–126.

James, T. S., Robin, C., Henton, J. A. and Craymer, M., 2021. *Relative sea-level projections for Canada based on the IPCC Fifth Assessment Report and the NAD83v70VG national crustal velocity model* [online]. Available from: https://ostrnrcan-dostrncan.canada.ca/handle/1845/138626.

James, T. S., Simon, K. M., Forbes, D. L., Dyke, A. S. and Mate, D. J., 2011. Sea-level Projections for Five Pilot Communities of the Nunavut Climate Change Partnership; Geological Survey of Canada, Open File 6715. [online], 23. Available from: http://gsc.nrcan.gc.ca/bookstore_e.php.

Johnson, K. and Arnold, E., 2010. Climate Change Adaptation Action Plan for Kugluktuk. [online], 109. Available from: https://www.climatechangenunavut.ca/en/resources/publications.

Jones, B. M., Farquharson, L. M., Baughman, C. A., Buzard, R. M., Arp, C. D., Grosse, G., Bull, D. L., Günther, F., Nitze, I., Urban, F., Kasper, J. L., Frederick, J. M., Thomas, M., Jones, C., Mota, A., Dallimore, S., Tweedie, C., Maio, C., Mann, D. H., Richmond, B., Gibbs, A., Xiao, M., Sachs, T., Iwahana, G., Kanevskiy, M. and Romanovsky, V. E., 2018. A decade of remotely sensed observations highlight complex processes linked to coastal permafrost bluff erosion in the Arctic. *Environmental Research Letters*, 13 (11).

Khanarmuei, M., Mardani, N., Suara, K. A., Sumihar, J., McCallum, A., Sidle, R. C. and Brown, R. J., 2020. Impact of sensor location on assimilated hydrodynamic model performance. *In*: *22nd Australasian Fluid Mechanics Conference, AFMC 2020*. Australasian Fluid Mechanics Society.

Kim, J., Murphy, E., Nistor, I., Ferguson, S. and Provan, M., 2021. Numerical analysis of storm surges on Canada's western arctic coastline. *Journal of Marine Science and Engineering*, 9 (3).

Krien, Y., Testut, L., Islam, A. K. M. S., Bertin, X., Durand, F., Mayet, C., Tazkia, A. R., Becker, M., Calmant, S., Papa, F., Ballu, V., Shum, C. K. and Khan, Z. H., 2017. Towards improved storm surge models in the northern Bay of Bengal. *Continental Shelf Research*, 135, 58–73.

Lenstra, K. J. H., Pluis, S. R. P. M., Ridderinkhof, W., Ruessink, G. and van der Vegt, M., 2019. Cyclic channel-shoal dynamics at the Ameland inlet: the impact on waves, tides, and sediment transport. *Ocean Dynamics*, 69 (4), 409–425.

Liew, M., Xiao, M., Farquharson, L., Nicolsky, D., Jensen, A., Romanovsky, V., Peirce, J., Alessa, L., McComb, C., Zhang, X. and Jones, B., 2022. Understanding Effects of Permafrost Degradation and Coastal Erosion on Civil Infrastructure in Arctic Coastal Villages: A Community Survey and Knowledge Co-Production. *Journal of Marine Science and Engineering*, 10 (3).

Liew, M., Xiao, M., Jones, B. M., Farquharson, L. M. and Romanovsky, V. E., 2020. Prevention and control measures for coastal erosion in northern high-latitude communities: A systematic review based on Alaskan case studies. *Environmental Research Letters*, 15 (9).

Magnan, A. K., Oppenheimer, M., Garschagen, M., Buchanan, M. K., Duvat, V. K. E., Forbes, D. L., Ford, J. D., Lambert, E., Petzold, J., Renaud, F. G., Sebesvari, Z., van de Wal, R. S. W., Hinkel, J. and Pörtner, H.-O., 2022. Sea level rise risks and societal adaptation benefits in low-lying coastal areas. *Scientific Reports* [online], 12 (1), 1–22. Available from: https://doi.org/10.1038/s41598-022-14303-w.

Manson, G. K., Davidson-arnott, R. G. D. and Forbes, D. L., 2015. Modelled nearshore sediment transport in open-water conditions , central north shore of Prince Edward Island, Canada, (November 2015), 101–118.

Obu, J., Lantuit, H., Grosse, G., Günther, F., Sachs, T., Helm, V. and Fritz, M., 2016. Coastal erosion and mass wasting along the Canadian Beaufort Sea based on annual airborne LiDAR elevation data. *Geomorphology* [online]. Available from: http://dx.doi.org/10.1016/j.geomorph.2016.02.014.

Overeem, I., Nienhuis, J. H. and Piliouras, A., 2022. Ice-dominated Arctic deltas.

Pertiwi, A. P., Roth, A., Schaffhauser, T., Bhola, P. K., Reuß, F., Stettner, S., Kuenzer, C. and Disse, M., 2021. Monitoring the spring flood in lena delta with hydrodynamic modeling based on sar satellite products. *Remote Sensing*, 13 (22), 1–19.

Prno, J., Bradshaw, B., Wandel, J., Pearce, T., Smit, B. and Tozer, L., 2011. Community vulnerability to climate change in the context of other exposure-sensitivities in Kugluktuk, Nunavut. *Polar Research*, 30 (SUPPL.1).

Scharffenberg, K. C., Whalen, D., Macphee, S. A., Marcoux, M., Iacozza, J., Davoren, G. and Loseto, L. L., 2019. Oceanographic, ecological, and socio-economic impacts of an unusual summer storm in the Mackenzie Estuary. *Arctic Science*, 6 (2), 62–76.

Sinitsyn, A. O., Guegan, E., Shabanova, N., Kokin, O. and Ogorodov, S., 2019. Fifty four years of coastal erosion and hydrometeorological parameters in the Varandey region, Barents Sea. *Coastal Engineering* [online], 157, 103610. Available from: https://doi.org/10.1016/j.coastaleng.2019.103610.

Smith, I. R., 2014. Reconnaissance assessment of landscape hazards and potential impacts of future climate change in Kugluktuk, western Nunavut. *Canada-Nunavut Geoscience Office Summary of Activities 2013 Summary of Activities 2013* [online], 149–158. Available from: http://cngo.ca/summary-of-activities/2013/.%0Ahttp://cngo.ca/summary-of-activities/2013/.

Smith, N. and Sattineni, A., 2016. Effect of Erosion in Alaskan Coastal Villages. [online], (1), 3. Available from: http://ascpro.ascweb.org/chair/paper/CPRT151002016.pdf.

Tejedor, A., Longjas, A., Caldwell, R., Edmonds, D. A., Zaliapin, I. and Foufoula-Georgiou, E., 2016. Quantifying the signature of sediment composition on the topologic and dynamic complexity of river delta channel networks and inferences toward delta classification. *Geophysical Research Letters*, 43 (7), 3280–3287.

Wilson, L., Owen, J., Bishop, B. and Fanning, L., 2021. *Key issues affecting coastal aquatic ecosystems and changing coastal conditions in Nunavut : A comparative assessment of five communities in the Kitikmeot region*.

Yamagami, A., Matsueda, M. and Tanaka, H. L., 2017. Extreme Arctic cyclone in August 2016. *Atmospheric Science Letters*, 18 (7), 307–314.

Ye, F., Zhang, Y. J., Wang, H. V., Friedrichs, M. A. M., Irby, I. D., Alteljevich, E., Valle-Levinson, A., Wang, Z., Huang, H., Shen, J. and Du, J., 2018. A 3D unstructured-grid model for Chesapeake Bay: Importance of bathymetry. *Ocean Modelling*, 127, 16–39.